

Inelastic electron scattering study of metallic oxidation: Synergistic effects involving electrons during the low temperature oxidation of Ni(111)

Wei Li, M. J. Stirniman, and S. J. Sibener

The James Franck Institute and Department of Chemistry, The University of Chicago, Chicago, Illinois 60637

(Received 24 October 1994; accepted 13 February 1995)

Oxygen adsorption and oxide growth on Ni(111) has been investigated at 120 K by high resolution electron energy loss spectroscopy (HREELS). We have found that an electron beam can stimulate nickel oxide growth at all incident electron energies examined, spanning the range from 5 eV to 2 keV. When electron irradiation is absent, oxidation occurs extremely slowly on this surface at low temperatures, resulting in mainly chemisorbed oxygen. We demonstrate that HREELS is capable of simultaneously monitoring oxide growth and characterizing the chemical nature of the oxygen/nickel interface, providing a useful complement to our earlier Auger spectroscopy based study of electron stimulated oxidation of this interface. We propose a model for the observed effect in which electrons create oxide nucleation centers on the Ni(111) surface in the presence of chemisorbed oxygen. This model allows us to quantitatively account for the data, including extraction of the relevant cross sections. © 1995 American Vacuum Society.

I. INTRODUCTION

Low energy electron beams have been used with increasing frequency in physical and chemical processes, such as electron beam lithography. The advent of the scanning tunneling microscope (STM) has made studies of electron-surface interactions even more important, due to its great potential in nanoengineering. It has been found that electron irradiation of surfaces can stimulate desorption,¹ adsorption,² dissociation,³ migration,⁴ adsorption site interchange,⁵ and oxidation,^{6,7} with electron stimulated desorption being the most extensively studied among these effects. In this article we report an important finding for the oxidation/corrosion behavior of Ni(111), namely that irradiation of the oxygen/Ni(111) interface by an electron beam at low substrate temperature leads to significant changes in the oxidation chemistry of this interface.

The oxidation of nickel surfaces has long been the subject of intensive study, with important implications for studies of metallic corrosion and catalysis. It is generally agreed that at room temperature oxygen uptake on nickel surfaces first proceeds through a fast chemisorption stage, followed by a relatively slow oxidation stage, with the nickel oxide overlayer reaching a thickness of three layers at saturation.⁸⁻¹⁰ More extensive oxidation can occur at elevated temperatures. While there have been many studies of high temperature oxidation, studies of oxide growth on nickel surfaces at low temperatures are rather scarce, but are in general agreement that the oxide grows more rapidly than at room temperature, and that the saturation oxygen uptake is about the same as for room temperature growth, i.e., 2 or 3 layers of nickel oxide.⁸⁻¹²

Recently, we have reinvestigated Ni(111) oxidation at 120 K. We have discovered, in contrast to previous work,⁸ that at this temperature nickel oxide growth proceeds extremely slowly (if at all) after completion of an initial oxygen chemisorption stage.¹³ We have found that electrons (examined from 5 eV to 2 keV) significantly enhance the oxidation of

the Ni(111) surface at 120 K,¹³ accounting for the discrepancy with previous results.⁸ Electron irradiation either during oxygen exposure, or alternating with it, can lead to this effect. In this article, we further characterize the electron stimulated oxidation effect by utilizing inelastic electron scattering. We demonstrate that high resolution electron energy loss spectroscopy (HREELS) is capable of both monitoring oxide growth and examining the chemical nature of the oxygen exposed interface.

To account for the experimental observations, we propose that the electron beam at the oxygen covered surface creates nucleation centers for nickel oxide growth at low temperature. A mechanistic model is put forward which quantitatively describes the data and yields relevant cross sections for the electron stimulated oxidation of this interface. The present finding has triggered reinvestigation of the kinetics and thermodynamics of oxide growth on nickel surfaces,¹⁴ and should lead to wide awareness of potential similar effects in other surface systems.

The ability of electrons to perturb experimental systems such that they deviate from their typical behavior has been well documented in the literature. For example, it has been reported for low energy electron diffraction (LEED) studies that electrons can cause the disordering of overlayers in some cases.¹⁵ This article will also demonstrate again the ability of electrons to alter experimental systems being investigated, at times so markedly that the conclusions drawn may not be directly applicable to the unperturbed system.

II. EXPERIMENT

The experiments were carried out in an ultrahigh vacuum (UHV) system (base pressure 7×10^{-11} Torr) that has been previously described.¹⁶ This apparatus has several surface diagnostics which have been used in this study, including LEED, Auger electron spectroscopy (AES), and high resolution electron energy loss spectroscopy (HREELS). The Ni(111) sample was oriented to within $\pm 0.2^\circ$ and prepared

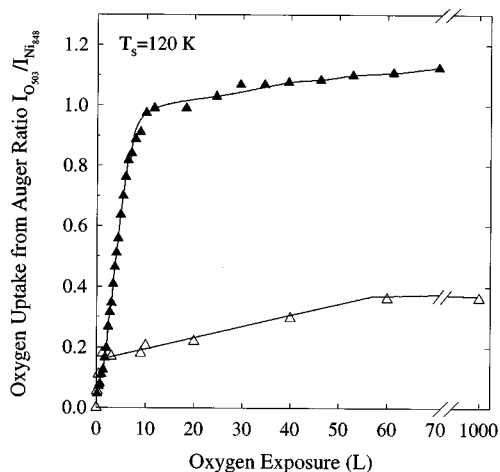


FIG. 1. Oxygen uptake vs oxygen exposure under various experimental conditions at 120 K. Solid triangles: Oxygen uptake during simultaneous exposure of the surface to both electrons and oxygen. Open triangles: Oxygen uptake without electron exposure. Electron beam conditions: $E_i=2$ keV, $I=2$ mA/cm².

by repeated cycles of Ar⁺ ion sputtering and annealing at 1100 K. Oxygen was admitted to the UHV chamber for background dosing at pressures of 3×10^{-8} to 3×10^{-7} Torr. Electron irradiation of the sample utilized the electron guns of the Auger spectrometer (for beam energies of 500 eV or higher) and LEED optics (for beam energies lower than 500 eV). The electron beam spot diameters were 1.4 mm for the Auger electron gun, and 1.4 to 2 mm for the LEED electron gun depending on electron energy. Beam current at the target was measured with the sample biased at +94 V to minimize secondary emission. Unless otherwise noted, all Auger measurements were done with a 2 keV electron beam with a current density of 2000 μ A/cm².

III. RESULTS

The observations which triggered the present work are shown in Figure 1. Here we measured the oxygen uptake of a Ni(111) surface at 120 K with AES. Data were collected using two different procedures. In the first case (Figure 1, solid triangles) the sample was simultaneously exposed to both oxygen and an electron beam from the Auger system's electron gun. Auger spectroscopy measurements were then performed at various exposure times in order to assess the extent of oxygen uptake by the sample. In the second case (Figure 1, open triangles) data were obtained by first dosing the sample to the desired oxygen exposure, and then measuring the oxygen content of the sample with AES. Then, before adsorbing oxygen to the next desired total oxygen exposure, the sample was first cleaned by sputtering and annealing. The utilization of this procedure ensured that the Ni(111) substrate was not subjected to electron irradiation at any time before or during oxygen exposure.

When dosing oxygen without electron irradiation at 120 K (Figure 1, open triangles), we find that following the initial chemisorption region there is very little further oxygen uptake, in contrast to earlier low temperature results.⁸ Moreover, even for very long exposure times, the saturation level

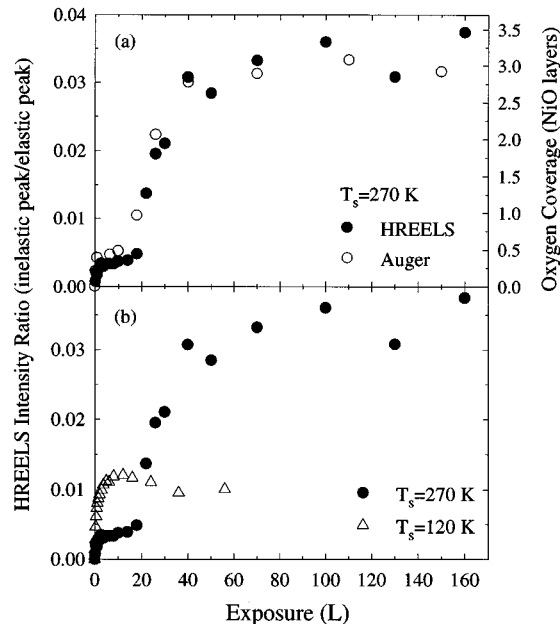


FIG. 2. (a) Oxygen uptake vs oxygen exposure at a surface temperature of 270 K, without electron irradiation. Open circles: Oxygen uptake from Auger intensity ratio of oxygen signal over nickel signal (the data have been converted to coverages, see the text); solid circles: HREELS intensity ratio of the nickel/oxygen inelastic (energy loss) peak to the elastic peak. (b) Oxygen uptake, measured by HREELS intensity ratios, as a function of oxygen exposure at 120 and 270 K without electron irradiation. HREELS spectrometer conditions: $E_i=7$ eV with $\theta_i=\theta_f=60^\circ$.

remains a factor of three lower than that previously reported.⁸ However, with electrons and oxygen simultaneously present we observe facile oxygen uptake, with a growth curve that reproduces previously reported low temperature oxygen incorporation data.⁸ We also observed that oxide growth at 270 K [open circles in Figure 2(a)] without electron irradiation reaches about the same level as that at 120 K with electron irradiation, which agrees quantitatively with previous findings for this system. In Figure 2(a), Auger intensities have been converted to nickel oxide coverage using a previously discussed electron escape depth correction.⁹ The agreement at 270 K, in spite of the presence of significant electron fluxes in the prior studies,⁸⁻¹⁰ suggests that synergistic effects involving electrons which modify the kinetics of oxidation become much less important for this interface near room temperature.¹⁴ A similar conclusion can be drawn from an earlier room temperature study¹⁷ involving polycrystalline and (110) oriented nickel.

Further evidence supporting the above observation is provided by measurements using HREELS, which also gives us the benefit of negligible perturbative effect of its electron beam due to its extremely low current density, 2.5 nA/cm². Figure 2(a) shows a comparison of the utility of AES and HREELS in monitoring the extent of oxygen uptake during oxygen exposure. HREELS spectra of oxygen on nickel surfaces exhibit an inelastic peak at about 70 meV energy loss.^{18,19} By comparing the intensity of this inelastic peak to the intensity of the specular elastic peak, we were able to duplicate the uptake curve produced by AES measurement¹³ for oxygen dosed at 270 K. The oxygen uptake curve ob-

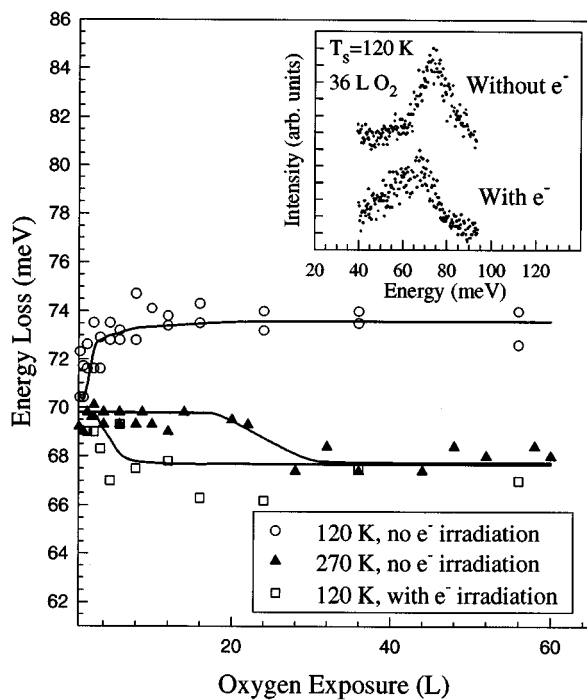


FIG. 3. Electron energy loss as a function of oxygen exposure under various oxygen dosing conditions. Open circles: oxygen dosed at 120 K; open squares: oxygen dosed at 120 K with 2 keV electron irradiation; solid triangles: oxygen dosed at 270 K. Inset: representative HREELS spectra used to generate data points in this figure; a spectral shift between the chemisorbed system and the oxidized metal can readily be seen. Spectrometer conditions: $E_i=7$ eV with $\theta_i=\theta_f=60^\circ$.

tained from HREELS measurements [Figure 2(a), solid circles] shows a rapid initial rise upon oxygen adsorption, corresponding to the chemisorption region in the AES oxygen uptake curve. This is followed by a plateau in the uptake curve out to about 20 langmuirs (L), corresponding to what is generally thought to be the oxide nucleation region. Finally, the HREELS oxygen uptake curve again rises quickly until saturation, showing the fast oxide growth stage and final thickening region. This excellent reproduction of the AES oxygen growth curve by the curve derived from HREELS intensity ratios shows HREELS intensity ratios to be an effective monitor of the oxidation process. Figure 2(b) shows a comparison of the oxidation behavior of this surface without electron irradiation at 270 and 120 K using the same method, i.e., monitoring the intensity ratio of the HREELS inelastic peak to the elastic peak. Figure 2(b) indicates that the oxygen uptake of this surface shows completely different behavior at 120 K than at 270 K, and the oxygen uptake at saturation at 120 K is much less than the saturation level at 270 K, in disagreement with the previous study.⁸

Perhaps the most informative chemical characterization of the nickel/oxygen interface comes from the energy shift of the inelastic scattering peak in HREELS measurements. In Figure 3, we present a plot of the peak energy loss in HREELS inelastic scattering as a function of oxygen exposure under various oxidation conditions. Figure 3 shows that when oxygen is dosed at a surface temperature of 120 K without the presence of electrons, upon saturation the loss peak stabilizes at about 73 meV, an energy which has been

previously assigned to the Ni–O stretch of atomically chemisorbed oxygen.^{18,19} However, if oxygen is dosed on the 270 K surface, or on the 120 K surface with 2 keV electron irradiation present, at saturation the inelastic scattering peaks occur at about 68 meV, a shift of 5 meV from the peak associated with chemisorbed oxygen. Similar energy losses in HREELS spectra for NiO grown on Ni(100) (Ref. 20), and for NiO(100) and (111) single crystals²¹ have been assigned to a surface optical phonon of NiO. These experimental values are in good agreement with the calculated energy of 68.3 meV for the Fuchs–Kliwer surface phonon of nickel oxide.²¹ We conclude that at 120 K and with electron irradiation we have formed 3 monolayers (ML) of NiO, whereas at 120 K and without electron irradiation essentially only chemisorbed oxygen is present, consistent with Figure 1.

We would like to point out that the data on the shift of the HREELS energy loss peaks presented in Figure 3 also contain important information about the oxide growth kinetics. In Figure 3 we have drawn three solid curves to guide the eye; these indicate the shift in the energy loss as a function of oxygen exposure for three oxygen dosing conditions. For the 120 K surface, the energy loss reaches the saturation value of 73 eV quickly during oxygen exposure, signaling prompt chemisorption, in agreement with the data in Figure 1 and Figure 2(b) (open triangles). On the other hand, when oxygen is dosed at a surface temperature of 270 K, the energy loss is a constant out to 20 L oxygen exposure, where it shifts to about 68 meV, indicating the onset of oxidation. This is consistent with the AES and HREELS uptake curves shown in Figure 2. As for oxidizing the 120 K surface with electron irradiation, the energy loss shifts down quickly to that of nickel oxide, indicating fast oxidation again in agreement with the AES data in Figure 1. To summarize, we find that the peak shift of the HREELS energy loss yields information on the oxidation kinetics consistent with that obtained by AES and the HREELS intensity ratios.

Oxidation data were also obtained by alternately exposing the sample to oxygen and then to a flux of electrons during Auger measurement of oxygen uptake. The oxygen flux was turned off during Auger data collection, ensuring that electrons and impinging oxygen were not present at the same time. The sample was then dosed with more oxygen and another Auger measurement subsequently taken. This process was continued until saturation. Two different oxidation procedures, one with electron irradiation and oxygen exposure occurring simultaneously, and the other with electron irradiation and oxygen exposure alternating during the course of oxidation, yield identical oxygen uptake behavior.

We have examined the electron stimulated oxidation effect over a wide range of electron energies. For these experiments, we set our electron guns (Auger gun for energy ≥ 500 eV, and LEED gun for energy < 500 eV) at the desired beam energy, and irradiated the surface with the electron beam during oxygen exposure. We have found that oxidation was stimulated by electron beams over the entire range of incident energies examined, 5 eV to 2 keV.

IV. DISCUSSION

Several key observations were considered in proposing a kinetic model for our results. Oxygen is known to adsorb dissociatively on Ni(111) above 20 K.²² We have also shown that it is not necessary to simultaneously expose the target surface to both electrons and molecular oxygen in order to grow nickel oxide at 120 K, and, in fact, a single exposure of a chemisorbed oxygen overlayer to a 20 sec dose of 2 keV electrons at $2000 \mu\text{A}/\text{cm}^2$ is sufficient to stimulate the growth of 3 ML of oxide upon subsequent oxygen exposure. Finally, we have found that electron irradiation of the clean Ni(111) surface using similar electron energies and currents does not promote low temperature oxidation. In light of these observations, we have ruled out electron induced dissociation of chemisorbed molecular oxygen, gas phase oxygen/electron interactions, and electron beam damage of the substrate as possible mechanisms. Further, other authors have shown that similar electron exposures lead to negligible surface heating,^{4,6} thus ruling out thermal effects.

Starting with the above view we have developed a kinetic model which provides an excellent description of our results, based on the premise that electrons create nucleation centers around which nickel oxide islands form and grow. We assume that the number of nucleation centers, N , created by the electrons follows a first order rate law:

$$\frac{dN}{dt} = (N_0 - N) \phi_e \sigma, \quad (1)$$

where N_0 is the saturation number of nucleation centers, ϕ_e is the electron flux density in electrons per cm^2 per second, and σ is the (energy dependent) cross section for the creation of nucleation centers by the electron beam. Using a simple first order kinetics model, we can describe the rate of nickel oxide growth as

$$\frac{d\theta}{dt} = k(\theta_s - \theta) \frac{N}{N_0}, \quad (2)$$

where θ is the oxide coverage, θ_s is saturation coverage, t is exposure time, and k is the rate constant for oxide growth around the nucleation centers. Integrating Eq. (2), with N/N_0 given by integrating Eq. (1), and subject to the initial condition $\theta = \theta_c$ at $t = 0$, where θ_c is the chemisorption saturation coverage and t is the oxygen exposure time, we have

$$\theta = \theta_s - (\theta_s - \theta_c) \exp \left[-k \left(t + \frac{1}{\phi_e \sigma} \exp(-\phi_e \sigma t) - \frac{1}{\phi_e \sigma} \right) \right]. \quad (3)$$

We have compared the results predicted by Eq. (3) to experimental curves of oxide growth as a function of electron beam current density for fixed oxygen exposure. Figure 4 presents Auger measurements of oxidation extent as a function of electron beam current density for incident beam energies of 30 eV [Figure 4(a)], 50 eV [Figure 4(b)], and 150, 500, and 2000 eV [Figure 4(c)]. Each data point in Figure 4 was obtained by exposing the 120 K surface to an electron beam at various current densities for 600 sec in the presence of 3×10^{-8} Torr oxygen. The solid lines in Figure 4 were obtained from nonlinear least squares fits of Eq. (3) to

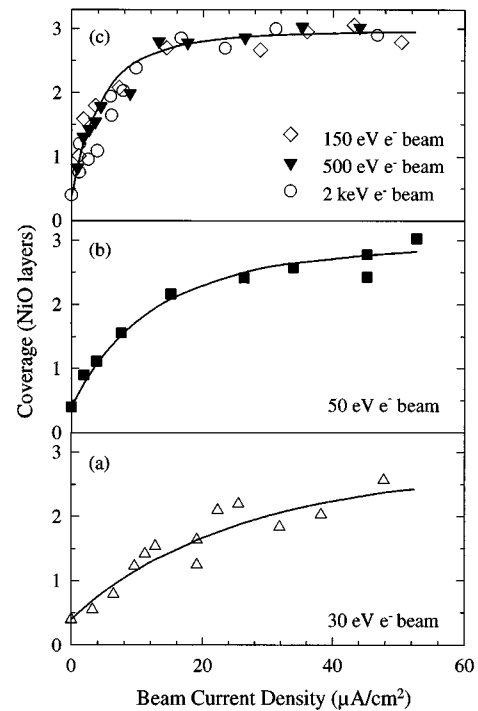


Fig. 4. Nickel oxide coverage vs electron beam current density for constant oxygen exposure time, $t = 600$ seconds at $P_{\text{ox}} = 3 \times 10^{-8}$ Torr. Electron beam energy: (a) 30 eV; (b) 50 eV; and (c) 150, 500, and 2000 eV. The solid lines are fits to the experimental data using Eq. (3); cross sections are given in the text.

the data, by varying only the energy dependent cross section for electron stimulated oxidation at the specified electron energy. Cross sections extracted from the fits are $5 \times 10^{-18} \text{cm}^2$ for 30 eV, $1 \times 10^{-17} \text{cm}^2$ for 50 eV, and $3 \times 10^{-17} \text{cm}^2$ for 150 eV, 500 eV, and 2 keV electrons.

Our model, using no adjustable parameters, can also quantitatively reproduce the oxygen uptake data obtained as a function of oxygen exposure at the fixed electron beam current density. As has been presented elsewhere,¹³ predictions from Eq. (3), using the cross section obtained from fits to Figure 4, agree well with oxygen uptake data taken with simultaneous oxygen and electron exposure using a 2 keV beam at current densities of 1.3, 9.8, and $2000 \mu\text{A}/\text{cm}^2$.

Recent studies have shown that oxide nucleation on Al(111) (Ref. 23) and Mg(0001) (Ref. 24) begins long before the saturation chemisorbed coverage is reached. While our HREELS and AES results show that at an oxygen coverage of 0.4 ML on Ni(111) the oxygen is predominately chemisorbed, some small amount of NiO may also be present. There is evidence of molecular oxygen adsorption on NiO thin films grown on Ni substrates²⁵ and single crystals of NiO.²⁶ This would raise the possibility of a surface O_2^- species as an intermediate in the formation of these nucleation centers. In fact, Chen *et al.*⁷ have observed stimulated oxidation on InP(110), and attributed it to the creation of O_2^- by electrons. Additionally, electronic excitation of chemisorbed atomic or molecular oxygen species could be a factor in the formation of these nucleation centers. The similarity of the oxidation behavior with and without electron irradiation at

room temperature suggests that the number of electron created nucleation centers is a decreasing function of temperature, and our results from a study of the temperature dependence of the electron stimulated oxidation effect support this speculation.¹⁴

V. CONCLUSION

In conclusion, we have demonstrated that synergistic effects involving incident fluxes of electrons can greatly modify the oxidation behavior of Ni(111) at low temperature. We have also shown that in the absence of such electrons nickel oxide grows much more slowly than had been previously reported for this important interface. We demonstrate that inelastic electron scattering can be used to simultaneously monitor the extent of oxygen uptake and the chemical nature of the surface oxygen species. We propose that the role of the electron is to create nucleation centers at which nickel oxide grows. A kinetic model has been proposed which quantitatively reproduces the electron stimulated oxidation data and yields the energy dependent cross sections for this phenomenon.

ACKNOWLEDGMENTS

This work was supported by the Air Force Office of Scientific Research and, in part, by the Materials Research Science and Engineering Center Program of the National Science Foundation at The University of Chicago under Award No. DMR-9400379.

¹R. Ramsier and J. T. Yates, Jr., Surf. Sci. Rep. **12**, 243 (1991).

²Y. Margoninski, D. Segal, and R. E. Kirby, Surf. Sci. **51**, 488 (1975).

³C. Xu and B. E. Koel, Surf. Sci. **292**, L803 (1993).

- ⁴H. J. Jansch, J. Xu, and J. T. Yates, Jr., J. Chem. Phys. **99**, 721 (1993).
- ⁵T. E. Madey, F. P. Netzer, J. E. Houston, D. M. Hanson, and R. Stockbauer, *Springer Series in Chemical Physics* (Springer, Heidelberg, 1983), Vol. 24, p. 120.
- ⁶J. M. Fontaine, O. Lee-Deacon, J. P. Duraud, S. Ichimura, and C. Le Gressus, Surf. Sci. **122**, 40 (1982).
- ⁷Y. Chen, Y. Luo, J. M. Seo, and J. H. Weaver, Phys. Rev. B **43**, 4527 (1991).
- ⁸P. H. Holloway and J. B. Hudson, Surf. Sci. **43**, 141 (1974).
- ⁹P. H. Holloway and J. B. Hudson, Surf. Sci. **43**, 123 (1974).
- ¹⁰P. R. Norton, R. L. Tapping, and J. W. Goodale, Surf. Sci. **65**, 13 (1977).
- ¹¹H. Hopster and C. R. Brundle, J. Vac. Sci. Technol. **16**, 548 (1979).
- ¹²W. Wang, N. Wu, and P. A. Thiel, J. Chem. Phys. **92**, 2025 (1990).
- ¹³W. Li, M. J. Stirniman, and S. J. Sibener, Surf. Sci. Lett. (in press).
- ¹⁴M. J. Stirniman, W. Li, and S. J. Sibener, J. Chem. Phys. (in press).
- ¹⁵A. G. Fedorus, V. V. Gouchar, I. V. Kanash, E. V. Klimenko, A. G. Naumovets, and I. N. Zaslomovich, Surf. Sci. **251/252**, 846 (1991).
- ¹⁶W. Menezes, P. Knipp, G. Tisdale, and S. J. Sibener, Phys. Rev. B **41**, 5628 (1990).
- ¹⁷J. Verhoeven and J. Los, Surf. Sci. **58**, 566 (1976); J. Verhoever, in *Proceedings of the VIIIth International Vacuum Congress and Third International Conference on Solid Surface*, edited by R. Dobrozemsky (International Union for Vacuum Science, Technique, and Applications, Vienna, 1977), p. 915.
- ¹⁸H. Ibach and D. Bruchmann, Phys. Rev. Lett. **44**, 36 (1980).
- ¹⁹G. Tisdale and S. J. Sibener, Surf. Sci. **311**, 360 (1994).
- ²⁰G. Dalmai-Imelik, J. C. Bertolini, and J. Rousseau, Surf. Sci. **63**, 67 (1977).
- ²¹P. A. Cox and A. A. Williams, Surf. Sci. **152/153**, 791 (1985).
- ²²J. D. Beckerle, Q. Y. Yang, A. D. Johnson, and S. T. Ceyer, Surf. Sci. **195**, 77 (1988).
- ²³H. Brune, J. Wintterlin, J. Trost, G. Ertl, J. Wiechers, and R. J. Behm, J. Chem. Phys. **99**, 2128 (1993).
- ²⁴P. A. Thiry, J. Ghijsen, R. Sporcken, J. J. Pireaux, R. L. Johnson, and R. Caudano, Phys. Rev. B **39**, 3620 (1989).
- ²⁵S. J. Bushby, T. D. Pope, B. W. Callen, K. Griffiths, and P. R. Norton, Surf. Sci. **256**, 301 (1991).
- ²⁶A. A. Tsyganenko, T. A. Rodionova, and V. N. Filimonov, React. Kinet. Catal. Lett. **11**, 113 (1979).